

Optimization of Synthesis Conditions for Urea-Formaldehyde Slow-Release Fertilizer Using Response Surface Methodology

Yanle Guo,^{||} Yiyun Shi,^{||} Shugang Zhang,* Zhenping Hao, Fengyuan Zhuang, Qiaobo Zhou, Hao Lu, and Qunxiang Cui*



Cite This: *ACS Omega* 2024, 9, 43477–43487



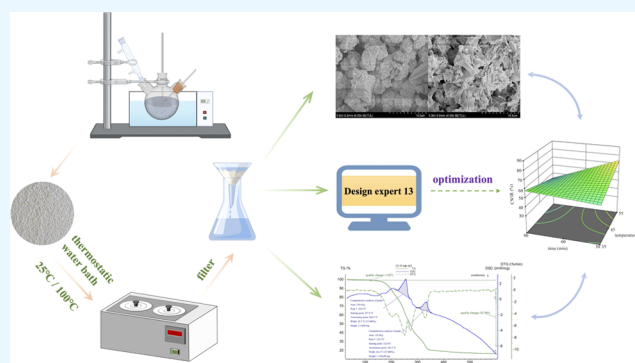
Read Online

ACCESS |

Metrics & More

Article Recommendations

ABSTRACT: In this study, we optimized the preparation of urea-formaldehyde fertilizer using response surface methodology with a Box–Behnken experimental design. The aim was to maximize the difference between CWIR and HWIR to maximize the content of slow-release insoluble nitrogen. In this work, a model of the impact of reaction factors on CWIR and HWIR was established. Through analysis of variance, the final model was significant. According to this model, the optimal reaction conditions were: a reaction temperature of 42.5 °C, a reaction time of 66.2 min, a U/F of 1.68, and a pH 3.3. Under these optimal conditions, the CWIR and HWIR reached 55.65 and 33.92%, respectively. In addition, the samples were characterized by scanning electron microscopy and thermal stability analysis. This study accurately synthesized urea-formaldehyde products with specific release periods according to



production needs in order to improve the efficiency of fertilizer utilization.

1. INTRODUCTION

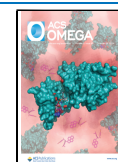
The latest survey by the Food and Agriculture Organization of the United Nations showed that the number of people affected by hunger globally had been increasing due to the multiple interrelated crises facing the global economy, and that the state of food security had deteriorated. Fertilizers have been indispensable in guaranteeing food security.^{1,2} However, due to the leaching, decomposition, and ammonium volatilization in soil, water, air, or other means, about 70% of traditional fertilizers cannot be directly utilized and are lost to the environment, thus causing environmental pollution.³ Slow-release fertilizer, which is a new type of fertilizer that coordinates its nutrient release mode with crop nutrient absorption, has attracted considerable attention as a replacement for traditional fertilizers,⁴ such as the urea-formaldehyde slow-release fertilizers that are widely used in agricultural production. As a long-term nitrogen fertilizer, urea-formaldehyde fertilizers have good slow-release performance and a nitrogen utilization rate of over 50%.^{5,6} They can improve the structural characteristics and permeability of soil and enhance the penetration of crop roots.

Urea-formaldehyde is a polymer obtained from the reaction of urea and formaldehyde under certain reaction conditions.⁷ The synthesis of urea-formaldehyde slow-release fertilizers is influenced by various reaction factors. Under different reaction temperatures, reaction times, molar ratios of urea/formaldehyde (U/F), and two-step pH conditions, there are significant

changes in the cold water insolubility rate (CWIR) and hot water insolubility rate (HWIR) of urea-formaldehyde slow-release fertilizers, and there are significant differences in their degree of polymerization.^{8,9} Therefore, to meet the fertilization demands of different crops, the fine synthesis of urea-formaldehyde products having specific release periods according to different reaction conditions is important to future development.

Most of the previous urea-formaldehyde synthesis research has focused on orthogonal experimental designs or single-factor tests, but their reaction process parameters have a wide range and there is no significant correlation with polymerization degree.^{2,10,11} The final optimization result may not be the optimal solution for urea-formaldehyde synthesis. To solve this problem, our research used multivariate statistical methods for optimization research, and an optimized mathematical response model for the synthesis of urea-formaldehyde fertilizer has been established.¹²

Received: May 23, 2024
Revised: October 7, 2024
Accepted: October 10, 2024
Published: October 17, 2024



Response surface methodology (RSM) is a technique that uses multivariate statistics to optimize process parameters and to improve experimental efficiency.¹³ RSM is used to accurately study the effects of various factors on specific variables by designing a few reasonable experiments, and determining the optimal conditions for multifactor experiments quickly and effectively.^{14,15} In recent years, RSM has been used in many fields of research such as electronics, machinery, agriculture, and the chemical industry.¹⁶ RSM has also been widely applied in the field of fertilizers, such as optimizing water-soluble slow-release nitrogen fertilizers for water-saving agriculture and optimizing biobased polyurethane, epoxy resin, and polyolefin wax composite coatings for controlled-release fertilizers.^{17,18} Based on previous research, this study uses RSM to explore the effects of different reaction factors on the synthesis of urea-formaldehyde from four perspectives—reaction temperature, reaction time, U/F, and pH—in order to determine the optimal conditions for the synthesis of urea-formaldehyde.

2. MATERIALS AND METHODS

2.1. Materials and Instruments. Urea was provided by Luxi Chemical Co., Ltd. (Shanghai, China). Formaldehyde solution (purity, 37%) was provided by Tianli Chemical Reagents Ltd. (Shanghai, China). NaOH solution (concentration, 2%), dilute sulfuric acid, and other reagents were all received from Tianjin Kaitong Chemical Reagents Co., Ltd. (Tianjin, China). The thermostat water bath was supplied by Shanghai Xinnuo Instrument Group Co., Ltd. (Shanghai, China). The drying oven was purchased from Shanghai Sunshine Scientific Instrument Co., Ltd. (Shanghai, China).

2.2. Synthesis of Urea-Formaldehyde. A urea and formaldehyde solution (37%) that was weighed on an analytical balance was added to a three-necked flask with a volume of 250 mL. The flask was then placed into an installed condenser tube and heated in a water bath. The first-step solution pH was adjusted to 9.0 by adding 2% NaOH. The reaction temperature and reaction time for each group were determined based on the experimental design. The processed samples were transferred from the flask to the beaker, and the two-step pH of the mixture was adjusted by adding dilute sulfuric acid. The entire solution was a dilute solution. After the white gelatinous viscous substance had settled, all the products were transferred from the beaker to a glass dish and dried in a drying oven for 3 h at a temperature of 90 °C. Finally, the urea-formaldehyde samples were ground into powder and sieved through a 0.9 mm standard sieve. The sieved samples were then placed in separate bottles. The preparation reaction equations for urea-formaldehyde are shown in Figure 1.

2.3. RSM Design. RSM was used to optimize the conditions for the synthesis of urea-formaldehyde fertilizer and to determine the optimal reaction conditions. The response variables were the CWIR and HWIR. The effects of the reaction temperature (X_1), reaction time (X_2), U/F (X_3), and two-step pH (X_4) on the CWIR and HWIR were investigated, as well as the interaction effects of these parameters on the CWIR and HWIR. The Box–Behnken design (BBD) consisted of three levels and four factors, which include influencing parameters and response variables, as shown in Table 1. The experimental scheme was designed using Design-Expert 13 software, and a total of 29 experiments were conducted.¹⁹ With this method, the parameter values were converted to values on a standardized scale, and the range for factorial points was from -1 to $+1$.²⁰ The center point was encoded as 0.²¹ The experimental design results

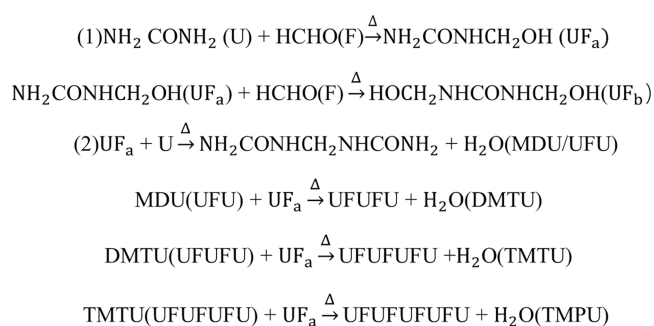


Figure 1. Synthesis reaction of urea-formaldehyde (MDU: methylenediurea; DMTU: dimethylenetriurea; TMTU: trimethylenetetraurea).

Table 1. Factors and Levels of Box–Behnken Design

coded	independent variable				response variable
	temperature (°C)	time (min)	U/F	pH	
−1	35	30	1.4	3	
0	45	60	1.55	4	CWIR
1	55	90	1.7	5	HWIR

of the RSM were analyzed using second-order polynomial (eq 1).

$$Y = \alpha_0 + \sum_{i=1}^n \alpha_i X_i + \sum_{i=1}^n \sum_{j=1}^n \alpha_{ij} X_i X_j + \varepsilon \quad (1)$$

where Y represents the response variable, α_0 indicates the regression coefficients for the intercept, α_i indicates linear interaction terms, and α_{ij} indicates quadratic interaction terms. The independent variables are X_i and X_j , ε is the statistical error, and n is the number of factors.

2.4. Determination of Urea-Formaldehyde. Two equal portions (2 g each) of each of the urea-formaldehyde samples were taken and placed in corresponding test tubes. Water in the amount of 20 mL was added to each test tube. One of the test tubes was placed in a constant-temperature water bath for 24 h, with the temperature set to 25 °C. Similarly, another test tube was placed in a constant-temperature water bath for 24 h, with the temperature set to 100 °C. After the 24 h extraction was completed, the samples were filtered. During the filtration process, water was filtered out, and substances that were insoluble in water were retained. After the filtration, the filter papers were dried in a 60 °C oven for 4 h. After they were dried, they were separately weighed. The equation for calculating the CWIR is as follows:

$$Y_1(\%) = \frac{b}{a} \times 100 \quad (2)$$

where b is the weight of undissolved substances in cold water (g), and a is the weight of the sample (g).

The equation for calculating the HWIR is as follows

$$Y_2(\%) = \frac{c}{a} \times 100 \quad (3)$$

where c is the weight of undissolved substances in hot water (g), and a is the weight of the sample (g).

2.5. Characterization of Typical Samples. Under the experimental conditions, samples 5, 16, and their corresponding extracted samples were representative, and the analysis of characteristic samples could provide references for subsequent

research. The characterization of samples may provide reference for further research. The structural morphology of the samples was examined using scanning electron microscopy (SEM; SU8020, Hitachi, Japan) at an accelerated voltage of 10 kV. Thermal stability analysis was carried out using a STA449F3 synchronous thermal analyzer (NETZSCH Group, Germany) in a nitrogen environment. The temperature range was RT to 600 °C, and the heating rate was 10 °C/min.

3. RESULTS AND DISCUSSION

The design and results of 29 experiments are shown in Table 2. To determine the significance of the different parameters on the

Table 2. Experimental Design and Results

trial	independent variables				response variables	
	X ₁ (°C)	X ₂ (min)	X ₃	X ₄	Y ₁ (%)	Y ₂ (%)
1	35	30	1.55	4	60	40
2	55	30	1.55	4	85	45
3	35	90	1.55	4	45	35
4	55	90	1.55	4	35	30
5	45	60	1.4	3	75	60
6	45	60	1.7	3	65	45
7	45	60	1.4	5	55	40
8	45	60	1.7	5	45	30
9	35	60	1.55	3	65	50
10	55	60	1.55	3	60	40
11	35	60	1.55	5	45	30
12	55	60	1.55	5	50	20
13	45	30	1.4	4	65	50
14	45	90	1.4	4	60	40
15	45	30	1.7	4	45	30
16	45	90	1.7	4	50	20
17	35	60	1.4	4	65	55
18	55	60	1.4	4	70	50
19	35	60	1.7	4	45	25
20	55	60	1.7	4	45	30
21	45	30	1.55	3	65	35
22	45	90	1.55	3	60	45
23	45	30	1.55	5	55	30
24	45	90	1.55	5	50	30
25	45	60	1.55	4	65	35
26	45	60	1.55	4	60	35
27	45	60	1.55	4	65	40
28	45	60	1.55	4	55	45
29	45	60	1.55	4	60	35

response values, regression analysis was conducted using analysis of variance (ANOVA) to evaluate the statistical analysis of the results and the acceptability of the model, as shown in Table 3.²² In the model, a *p*-value <0.05 was considered to be significant, and a *p*-value <0.01 was considered to be extremely significant. Moreover, we used the normal probability distribution map of residuals, the distribution map of predicted and actual values, and a three-dimensional response surface map to further verify the results and ensure consistency.²³ When we predicted the optimal conditions for the reaction, we repeated the test three times to ensure consistency.²⁴

3.1. Impact of Independent Variables on CWIR. Design-Expert 13 software was used to simulate the second-order models of the data. According to the significant variables in Table 3, the CWIR could be predicted through multiple regression analysis using eq 4.

Table 3. ANOVA for CWIR and HWIR^{af}

source		sum of squares	df	mean square	F-value	p-value
model	Y ₁	2291.67	10	229.17	4.17	0.0042
	Y ₂	2043.75	10	204.37	5.3	0.0010
X ₁	Y ₁	33.33	1	33.33	0.6064	0.4462
	Y ₂	33.33	1	33.33	0.8752	0.3619
X ₂	Y ₁	468.75	1	468.75	8.53	0.0091
	Y ₂	75.00	1	75.00	1.97	0.1775
X ₃	Y ₁	752.08	1	752.08	13.68	0.0016
	Y ₂	1102.08	1	1102.08	28.94	<0.0001
X ₄	Y ₁	675.00	1	675.00	12.28	0.0025
	Y ₂	752.08	1	752.08	19.75	0.0003
X ₁ X ₂	Y ₁	306.25	1	306.25	5.57	0.0297
	Y ₂	25.00	1	25.00	0.6564	0.4284
X ₁ X ₃	Y ₁	6.25	1	6.25	0.1137	0.7399
	Y ₂	25.00	1	25.00	0.6564	0.4284
X ₁ X ₄	Y ₁	25.00	1	25.00	0.4548	0.5086
	Y ₂	0.0000	1	0.0000	0.0000	1.0000
X ₂ X ₃	Y ₁	25.00	1	25.00	0.4548	0.5086
	Y ₂	0.0000	1	0.0000	0.0000	1.0000
X ₂ X ₄	Y ₁	0.0000	1	0.0000	0.0000	1.0000
	Y ₂	25.00	1	25.00	0.6564	0.4284
X ₃ X ₄	Y ₁	0.0000	1	0.0000	0.0000	1.0000
	Y ₂	6.25	1	6.25	0.1641	0.6902
residual	Y ₁	989.37	18	54.96		
	Y ₂	685.56	18	38.09		
lack of fit	Y ₁	919.37	14	65.67	3.75	0.1054
	Y ₂	605.56	14	43.25	2.16	0.2377
pure error	Y ₁	70.00	4	17.50		
	Y ₂	80.00	4	20.00		
cor total	Y ₁	3281.03	28			
	Y ₂	2729.31	28			

^aY₁: R² = 0.6985, Adj. R² = 0.5309, Adeq precision = 7.0265; Y₂: R² = 0.7488, Adj. R² = 0.6093, Adeq precision = 9.2048.

$$Y_1 = 57.41 + 1.67X_1 - 6.25X_2 - 7.92X_3 - 7.50X_4 - 8.75X_1X_2 - 1.25X_1X_3 + 2.50X_1X_4 + 2.50X_2X_3 \quad (4)$$

Here, Y₁ is the CWIR, and X₁, X₂, X₃, and X₄ are the independent variables.

In the ANOVA, the *F*-value and *p*-value directly represent the significance of the parameters and the degree to which each factor has a significant impact on the response (Table 3).²⁵ The *F*-value of the model was 4.17 with a very low probability (*p*-value = 0.0042 < 0.01), which indicated that the model was significantly well fit and had statistical significance. The regression coefficient R² was used to measure the strength of the relationship between the model and the dependent variable.²⁶ The R² was 0.6985, which indicated a fitting rate of 69.85% for the model, and the remaining 30.15% was influenced by other variables.²⁷ This result requires further study in the future. The lack of fit of the model was 0.1054 > 0.05, which was not significant and thus quite beneficial for the model. This result indicated that the response equation simulated the relationship between the independent variable and the response.²⁸ The adequate precision of the model was 7.0265 > 4, indicating that the model was suitable for predicting output responses and was considered reasonable.²⁹

For the CWIR, the distribution of the predicted and actual values was almost a straight line, which indicated that using the

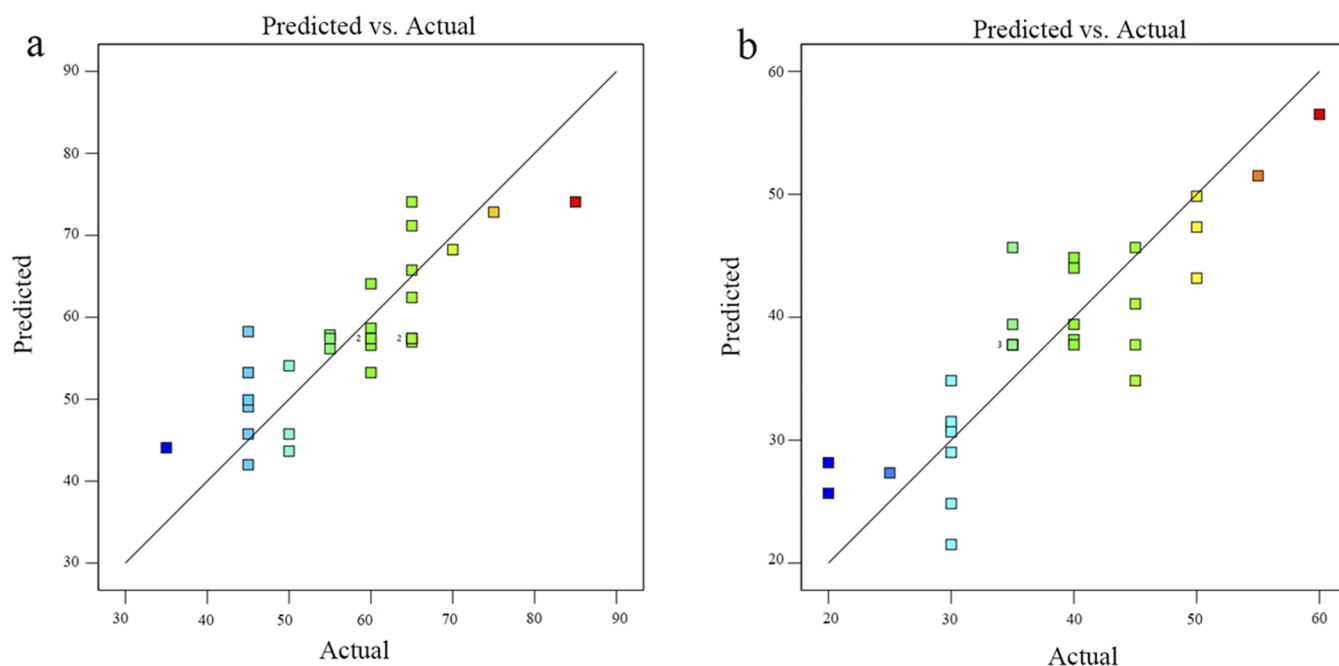


Figure 2. Distribution map of predicted values and actual values for cold water (a) and hot water (b) insolubility rates.

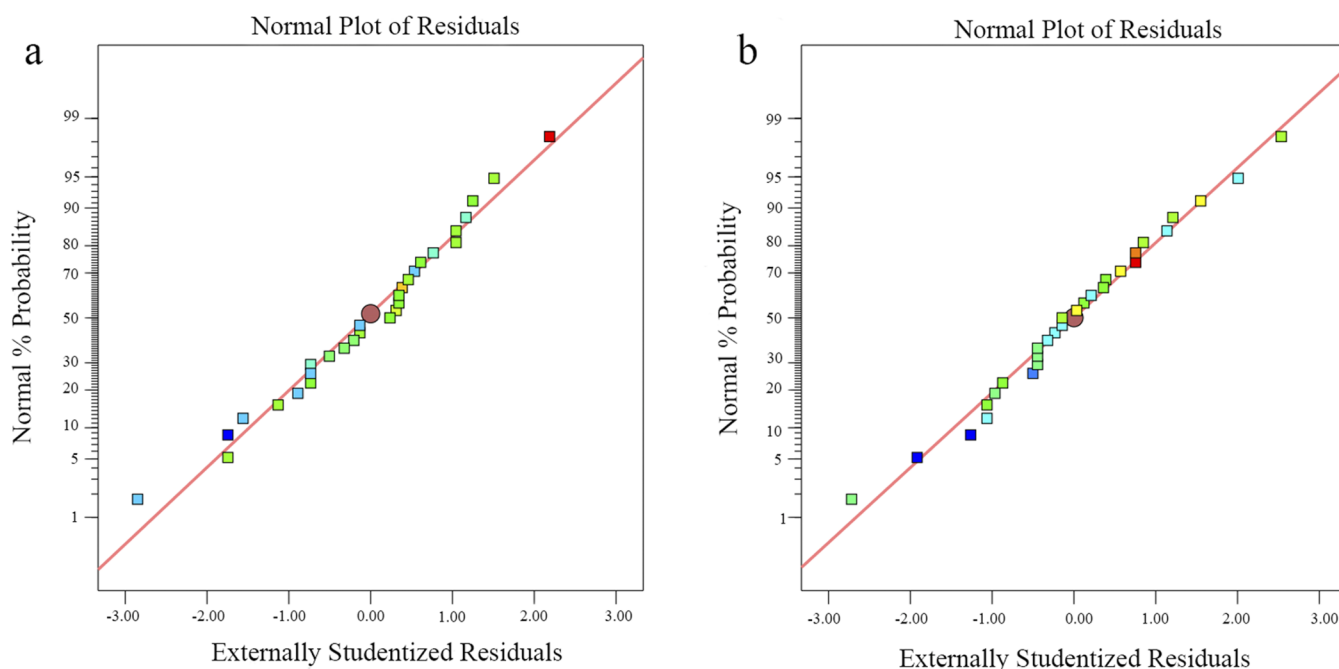


Figure 3. Normal probability distribution diagram of residuals for cold water (a) and hot water (b) insolubility rates.

RSM to fit the model had good adaptability (Figure 2a).³⁰ The residual normal distribution map is a useful method for judging the adaptability of a model in regression analysis. As shown in Figure 3a, the normal probability of the residuals was distributed along a straight line, which indicated that the model had good adaptability and that there was no response value that strongly deviated from normality.³¹

The regression model showed that the first-order terms X_2 , X_3 , and X_4 had a significant impact on the CWIR (p -value < 0.01). It has been used to analyze optimal conditions in systems with multifactor interaction analyses including among different factors, whereas the interaction term X_1X_2 had a significant impact on the CWIR (p -value < 0.05), which was not found ever.

The effect of the U/F on the CWIR was the most significant with an F -value of 13.68, followed by the pH and reaction time, and the reaction temperature was not significant. The order of factors affecting the CWIR was: U/F > pH > reaction time > reaction temperature.

3.2. Impact of Independent Variables on HWIR. The ANOVA clearly demonstrated the significance of the different parameters that affected the response values. According to Table 3, there was a significant relationship between the response value Y_2 and the independent variable (reaction factors).³² The interaction between the reaction temperature, reaction time, U/F, and pH on the HWIR is represented by eq 5

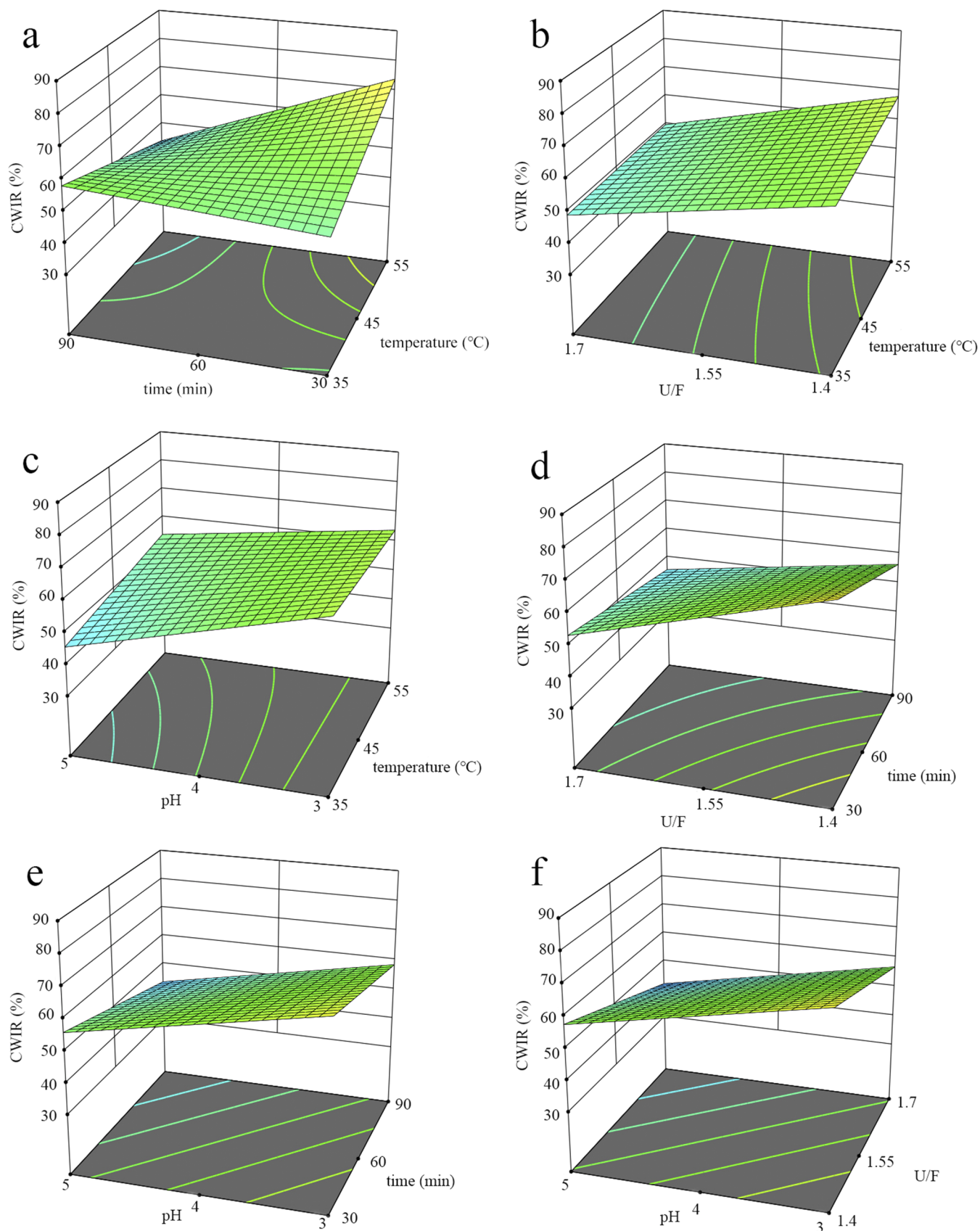


Figure 4. Impact of interaction terms on CWIR, (a) the interaction between time and temperature, (b) the interaction between U/F and temperature, (c) the interaction between pH and temperature, (d) the interaction between U/F and time, (e) the interaction between pH and time, (f) the interaction between pH and U/F.

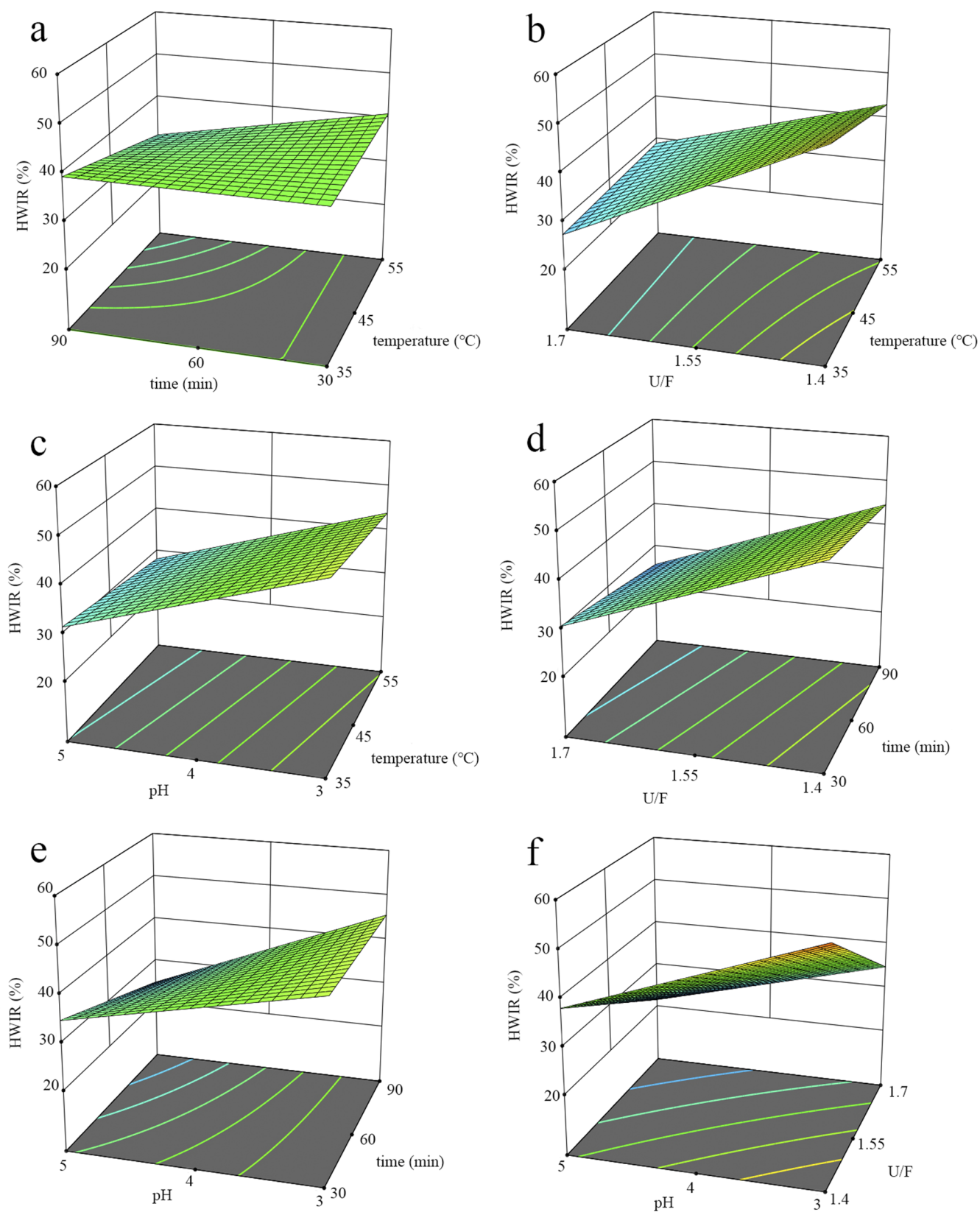


Figure 5. Impact of interaction terms on HWIR, (a) the interaction between time and temperature, (b) the interaction between U/F and temperature, (c) the interaction between pH and temperature, (d) the interaction between U/F and time, (e) the interaction between pH and time, (f) the interaction between pH and U/F.

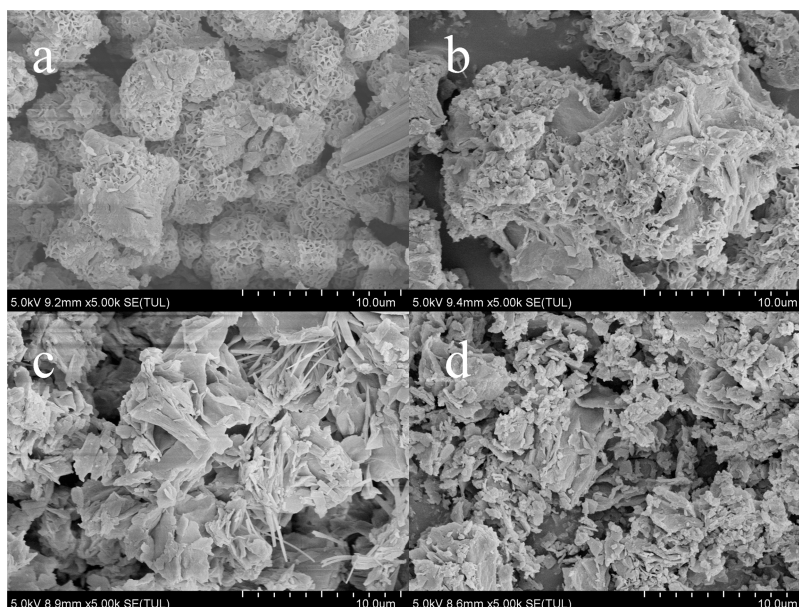


Figure 6. SEM images of the surface morphology of the (a) unextracted sample 5, (b) sample 5 after extraction (sample SE), (c) unextracted sample 16, and (d) sample 16 after extraction (sample 16E).

$$Y_2 = 37.76 - 1.67X_1 - 2.50X_2 - 9.58X_3 - 7.92X_4 - 2.50X_1X_2 + 2.50X_1X_3 - 2.50X_2X_4 + 1.25X_3X_4 \quad (5)$$

Here, Y_2 is the HWIR, and X_1 , X_2 , X_3 , and X_4 are the independent variables.

The larger the F -value and the smaller the p -value, the more significant the correlation coefficient.³³ According to the ANOVA (Table 3), the p -value of the model was $0.001 < 0.05$, which indicated that the model was significant. The lack of fit was not significant (p -value = $0.2377 > 0.05$), which indicated that the model fitted well with the experimental data and was appropriate.¹⁶ The multiple correlation coefficient R^2 was 0.7488, which meant that 25.12% of the analysis was not explained by the model.³⁴ Adequate precision was measured as the ratio of effective signal-to-noise, with an accuracy of $9.2084 > 4$, which was considered reasonable.³⁵

Figure 2b showed a comparison between the predicted and actual values, and the distribution of the predicted and actual values was almost a straight line, indicating that the use of RSM to fit the model had good adaptability. The residual normal distribution map is an important tool of the RSM to determine the adaptability of fitted models.³⁶ For the HWIR, the normal probability of residuals followed a linear distribution, which indicated that the model had good adaptability (Figure 3b).

From the ANOVA, it can be seen that the p -values of the primary terms X_3 and X_4 were less than 0.01, which indicated a significant impact on the HWIR, whereas the other factors were not significant. X_3 was the most significant factor that affected the synthesis of urea-formaldehyde fertilizer (p -value < 0.0001).^{13,37} The order of factors affecting the HWIR was: $U/F > pH > reaction\ time > reaction\ temperature$.

3.3. Effects and Optimization of Reaction Conditions on CWIR and HWIR. The interactions and optimal values of variables were determined using RSM, and the three-dimensional response surface plots were intuitive (Figures 4 and 5). The three-dimensional response surface plots were generated by

using a predictive model, which was able to intuitively and clearly represent the interaction between parameters.³⁸

Clearly, the CWIR decreased with an increase in the U/F . From the reaction formula (Figure 1), it could be seen that the smaller the U/F , the more formaldehyde there was, which was conducive to the progress of the reaction. The concentration of insoluble nitrogen in the cold water was lower at $U/F = 1.7$ than at $U/F = 1.4$.

The CWIR decreased with an increase in pH . A low pH value was beneficial for the condensation reaction of the entire reaction system. The lower the pH of urea-formaldehyde, the more $HNCH_2N(CH_2)$ were formed, and the higher the curing conversion rate. So in the methylation reaction stage, when the pH was adjusted to 3, urea-formaldehyde precipitates quickly. Therefore, a large amount of insoluble urea-formaldehyde condensate was formed,³⁹ which increased the content of insoluble nitrogen in cold water. According to the CWIR, the molar ratio of urea/formaldehyde had the greatest impact on the insoluble nitrogen in urea-formaldehyde products and was followed by pH . In this study, the changes in reaction temperature and reaction time did not have a significant impact on the CWIR, and this finding was similar to previous research findings.^{12,40} Meanwhile, the interaction between the reaction temperature and the reaction time was not significant.

In strong acidic environments, the HWIR of the samples were relatively low. The reason for this was that under strong acid conditions, the hydroxymethylation products (obtained from the hydroxymethylation reaction) quickly synthesized into methylene products. The increase of methylene products accelerated the methylation reaction. As the chain length of the product increased, the proportion of hot water insoluble nitrogen in the obtained product increased.⁴¹

The effect of temperature on the HWIR was not significant. During the hot water extraction process, small molecules gradually dissolved under conditions of increasing temperature, which left only large molecules that were not soluble in water in the sample.

As the U/F increased, the HWIR significantly decreased. The U/F had the most significant effect on the HWIR, followed by

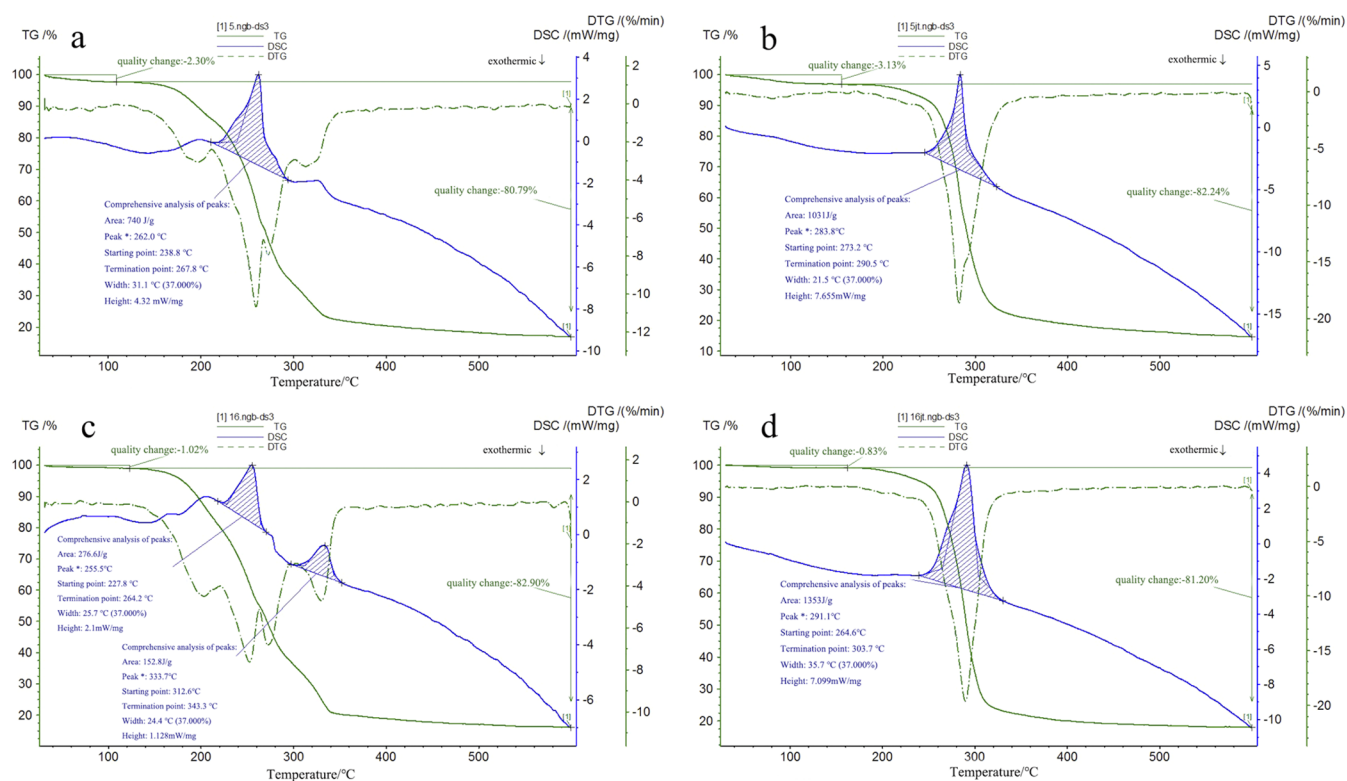


Figure 7. TGA analysis of (a) unextracted sample 5, (b) sample 5 after extraction (sample 5E), (c) unextracted sample 16, and (d) sample 16 after extraction (sample 16E).

the pH. In this study, the changes in reaction temperature and reaction time did not have a significant effect on the insoluble nitrogen in hot water.⁴²

3.4. Characteristics. **3.4.1. SEM Analysis.** Samples 5 and 16 showed significant differences in their HWIR. Therefore, samples 5, 16, and their corresponding samples after hot water extraction (sample 5E, sample 16E) were selected for microscopic morphology detection to further compare the size of the molecules in the different samples. The SEM images of sample 5, sample 16, sample 5E, and sample 16E are shown in Figure 6. Sample 5 was blocky in shape, with a relatively dense surface, fewer pores and a smaller specific surface area (Figure 6a,b).⁴³ Sample 16 had a loose and rough surface with numerous pores, resulting in a larger specific surface area (Figure 6c,d).⁴⁴ There was no significant difference between the surface structure of the hot water extracted sample and that of the nonextracted sample. This indicated that the effect of temperature on the HWIR was not significant, and that the dissolution of small molecules had no significant effect on the overall structure, which was consistent with the analysis in Section 3.3.

3.4.2. Thermal Stability Analysis. Characteristic samples 5, 16, and their corresponding samples after hot water extraction (sample 5E, sample 16E) were selected for TG-DSC analysis. The differences in the thermodynamic stability of the extracted and unextracted samples were studied, and the results are shown in Figure 7.

The DTG curve represents the decomposition rate of a sample. There are differences in the curve shape between the unextracted samples and the extracted samples. This may be because the unextracted sample contains unreacted urea and some small molecule substances. After the extraction, the small molecules dissolved in water and did not remain in the sample, whereas the undissolved large molecules remained.

According to the DSC heat absorption curve, the endothermic peak areas of unextracted samples 5 and 16 were 740 and 429.4 J/g, respectively. After hot water extraction, the endothermic peak areas of samples 5E and 16E were 1031 and 1353 J/g. The endothermic peak area of the sample after hot water extraction was much larger than that of the unextracted sample, which indicated that the decomposition process of the extracted sample required more heat for the same mass. This might have been due to the high purity of macromolecular substances in the extracted sample, which were difficult to dissolve.

The endothermic temperature starting points of unextracted samples 5 and 16 were 238.8 and 227.8 °C, respectively. After the hot water extraction, the endothermic temperature starting points of samples 5E and 16E were 273.2 and 264.4 °C, respectively. The endothermic temperature starting points of the unextracted sample were earlier than those of the sample after hot water extraction. This might have been due to the presence of unreacted urea and small molecule substances in the unextracted sample, which decomposed at a lower temperature.

3.5. Model Validation. Compared to single factor and orthogonal experiments, the test can only be optimized for one variable at a time or obtain the relative optimal solutions of different variables and limited light combinations, Design-Expert software is able to optimize models while considering and finding the optimal combination of variable levels.⁴⁵ Target values were selected for four independent variables: reaction temperature, reaction time, U/F, and pH. The purpose of this was to select the optimal value through the BBD of RSM and to maximize the content of insoluble nitrogen in cold water and minimize the content of insoluble nitrogen in hot water, thereby improving the content of slow-release insoluble nitrogen.⁴⁶ The optimal conditions for synthesizing urea-formaldehyde were optimized using this software, and the results showed that the

optimal reaction temperature was 42.5 °C, optimal reaction time was 66.2 min, optimal U/F was 1.68, and optimal pH was 3.3. Under these conditions, the CWIR reached 55.65% and the HWIR reached 33.92%. To verify the accuracy of the response surface optimization values, urea-formaldehyde fertilizer was prepared under the above conditions. The results showed that the CWIR was 58.17% and the HWIR was 31.85%. There was a good correlation between the experimental results and the predicted values, and the model was able to effectively predict the level of response values.

4. CONCLUSIONS

This study used RSM and BBD to discuss and study the effects of reaction temperature, reaction time, U/F, and pH on the CWIR and HWIR. The BBD of RSM successfully maximized the insoluble nitrogen content in cold water and minimized the insoluble nitrogen content in hot water, thereby increasing the content of slow-release insoluble nitrogen. The BBD consisted of three levels and four variables. The response surface optimization experiments showed that the U/F and pH had the most significant impact on the CWIR and HWIR, whereas the reaction temperature and time were negligible parameters. The experimental variables were set to a reaction temperature of 42.5 °C, reaction time of 66.2 min, U/F of 1.68, and pH of 3.3, which resulted in the best reaction results. Under these conditions, the CWIR and HWIR reached 55.65 and 33.92%, respectively. This study showed that the BBD using RSM served as a successful optimization model for urea-formaldehyde synthesis that could help to accurately synthesize urea-formaldehyde products having specific release periods. Meanwhile, optimizing the synthesis of urea-formaldehyde fertilizer may further provide a basis for fertilizer production and improve its slow-release performance. This article only considered the sustained release effect of ultrafiltration under hydroponic conditions. The impact of different soil types or crop cultivation conditions on fertilizer response also be considered in further research in the future. And this modeling article was precisely providing model support for further in-depth exploration, in order to better synthesize UF products with different characteristics, and then carried out experimental research such as soil cultivation.

AUTHOR INFORMATION

Corresponding Authors

Shugang Zhang – National Engineering Laboratory for Efficient Utilization of Soil and Fertilizer Resources, National Engineering & Technology Research Center for Slow and Controlled Release Fertilizers, College of Resources and Environment, Shandong Agricultural University, Tai'an 271018, China; orcid.org/0000-0002-1428-9082; Email: shugangzhang2014@163.com

Qunxiang Cui – College of Horticulture and Landscape Architecture, Jinling Institute of Technology, Nanjing 210038, China; orcid.org/0009-0002-9579-6517; Phone: +86-025-85393314; Email: le130103@126.com

Authors

Yanle Guo – College of Horticulture and Landscape Architecture, Jinling Institute of Technology, Nanjing 210038, China; orcid.org/0000-0003-0134-377X

Yiyun Shi – College of Horticulture and Landscape Architecture, Jinling Institute of Technology, Nanjing 210038, China

Zhenping Hao – College of Horticulture and Landscape Architecture, Jinling Institute of Technology, Nanjing 210038, China

Fengyuan Zhuang – College of Horticulture and Landscape Architecture, Jinling Institute of Technology, Nanjing 210038, China

Qiaobo Zhou – College of Horticulture and Landscape Architecture, Jinling Institute of Technology, Nanjing 210038, China

Hao Lu – Key Laboratory of Crop Genetics and Physiology of Jiangsu Province, Co-Innovation Center for Modern Production Technology of Grain Crops of Jiangsu Province, Yangzhou University, Yangzhou 225009, China

Complete contact information is available at:

<https://pubs.acs.org/10.1021/acsomega.4c04847>

Author Contributions

[†]Y.G. and Y.S. authors contributed equally to this work.

Notes

The authors declare no competing financial interest.

ACKNOWLEDGMENTS

This research was funded by the Jiangsu Seed Industry Revitalization Project [JBGS(2021)015], and the Colleges and Universities in Jiangsu Province Natural Science Foundation of China (19KJB210014), and the Jiangsu Seed Industry Revitalization Project [JBGS(2021)074], and the Dr. Startup Project of Jinling Institute of Technology (jit-b-201915). We also thank Junshan Guo for technical assistance and Ailing Song for reviewing this manuscript.

REFERENCES

- (1) Shen, Y.; Wang, H.; Li, W.; Liu, Z.; Liu, Y.; Wei, H.; Li, J. Synthesis and characterization of double-network hydrogels based on sodium alginate and halloysite for slow release fertilizers. *Int. J. Biol. Macromol.* **2020**, *164*, 557–565.
- (2) Vejan, P.; Khadiran, T.; Abdullah, R.; Ahmad, N. Controlled release fertilizer: A review on developments, applications and potential in agriculture. *J. Controlled Release* **2021**, *339*, 321–334.
- (3) Duan, Q.; Jiang, S.; Chen, F.; Li, Z.; Ma, L.; Song, Y.; Yu, X.; Chen, Y.; Liu, H.; Yu, L. Fabrication, evaluation methodologies and models of slow-release fertilizers: A review. *Ind. Crops Prod.* **2023**, *192*, No. 116075.
- (4) Nardi, P.; Neri, U.; Di Matteo, G.; Trinchera, A.; Napoli, R.; Farina, R.; Subbarao, G. V.; Benedetti, A. Nitrogen Release from Slow-Release Fertilizers in Soils with Different Microbial Activities. *Pedosphere* **2018**, *28* (2), 332–340.
- (5) Yamamoto, C. F.; Pereira, E. I.; Mattoso, L. H. C.; Matsunaka, T.; Ribeiro, C. Slow release fertilizers based on urea/urea–formaldehyde polymer nanocomposites. *Chem. Eng. J.* **2016**, *287*, 390–397.
- (6) Liu, Y.; Li, J.; Ma, R.; Dong, Y.; Huang, S.; Sao, J.; Jiang, Y.; Ma, L.; Cheng, D. Determination of Residual Formaldehyde in Urea-Formaldehyde Fertilizer and Formaldehyde Release from Urea-Formaldehyde Fertilizer During Decomposition. *J. Polym. Environ.* **2020**, *28* (8), 2191–2198.
- (7) Xiang, Y.; Ru, X.; Shi, J.; Song, J.; Zhao, H.; Liu, Y.; Zhao, G. Granular, Slow-Release Fertilizer from Urea-formaldehyde, Ammonium Polyphosphate, and Amorphous Silica Gel: A New Strategy Using Cold Extrusion. *J. Agric. Food Chem.* **2018**, *66* (29), 7606–7615.
- (8) Giroto, A. S.; do Valle, S. F.; Guimaraes, G. G. F.; Jablonowski, N. D.; Ribeiro, C.; Mattoso, L. H. C. Different Zn loading in Urea-Formaldehyde influences the N controlled release by structure modification. *Sci. Rep.* **2021**, *11* (1), No. 7621.
- (9) Cassim, B. M. A. R.; Machado, A. P. M.; Fortuna, D.; Moreira, F. R.; Zampar, E. J. D. O.; Batista, M. A. Effects of Foliar Application of

Urea and Urea-Formaldehyde/Triazone on Soybean and Corn Crops. *Agronomy* **2020**, *10* (10), 1549.

(10) Jahns, T.; Ewen, H.; Kaltwasser, H. Biodegradability of urea-aldehyde condensation products. *J. Polym. Environ.* **2003**, *11*, 155–159.

(11) Maslosh, V. Z.; Kotova, V. V.; Maslosh, O. V. Influence of process factors on the structure of urea-formaldehyde resin. *Russ. J. Appl. Chem.* **2003**, *76* (3), 483–486.

(12) Guo, Y.; Zhang, M.; Liu, Z.; Tian, X.; Zhang, S.; Zhao, C.; Lu, H. Modeling and Optimizing the Synthesis of Urea-formaldehyde Fertilizers and Analyses of Factors Affecting these Processes. *Sci. Rep.* **2018**, *8* (1), No. 4504.

(13) Sadidi, M.; Hajilary, N.; Abbasi, F. Optimization of biofuel dehydration performance of PES/PEI/MXene membrane by response surface method. *J. Environ. Chem. Eng.* **2023**, *11* (5), No. 110946.

(14) Yang, X.; Zhang, H.; Cheng, S.; Zhou, B. Optimization of the adsorption and removal of Sb(III) by MIL-53(Fe)/GO using response surface methodology. *RSC Adv.* **2022**, *12* (7), 4101–4112.

(15) Chen, W.-H.; Uribe, M. C.; Kwon, E. E.; Lin, K.-Y. A.; Park, Y.-K.; Ding, L.; Saw, L. H. A comprehensive review of thermoelectric generation optimization by statistical approach: Taguchi method, analysis of variance (ANOVA), and response surface methodology (RSM). *Renewable Sustainable Energy Rev.* **2022**, *169*, No. 112917.

(16) Hu, J.; Li, A. Analysis of Factors Affecting Polymer Flooding Based on a Response Surface Method. *ACS Omega* **2021**, *6* (14), 9362–9367.

(17) Guo, Y.; Zhang, M.; Liu, Z.; Zhao, C.; Lu, H.; Zheng, L.; Li, Y. C. Applying and optimizing water-soluble, slow-release nitrogen fertilizers for water-saving agriculture. *ACS Omega* **2020**, *5* (20), 11342–11351.

(18) Tian, H.; Liu, Z.; Zhang, M.; Guo, Y.; Zheng, L.; Li, Y. C. Biobased polyurethane, epoxy resin, and polyolefin wax composite coating for controlled-release fertilizer. *ACS Appl. Mater. Interfaces* **2019**, *11* (5), 5380–5392.

(19) Athar, M.; Zaidi, S.; Hassan, S. Z. Intensification and optimization of biodiesel production using microwave-assisted acid-organocatalyzed transesterification process. *Sci. Rep.* **2020**, *10* (1), No. 21239.

(20) Darvishmotevalli, M.; Zarei, A.; Moradnia, M.; Noorisepehr, M.; Mohammadi, H. Optimization of saline wastewater treatment using electrochemical oxidation process: Prediction by RSM method. *MethodsX* **2019**, *6*, 1101–1113.

(21) Yolmeh, M.; Jafari, S. M. Applications of Response Surface Methodology in the Food Industry Processes. *Food Bioprocess Technol.* **2017**, *10* (3), 413–433.

(22) Chikati, R.; Mpandanyama, T. A.; Nkazi, D.; Khangale, P.; Gorimbo, J. Optimization and evaluation of the distribution of Fischer–Tropsch products over a cobalt-based catalyst utilizing design expert software. *Heliyon* **2024**, *10* (1), No. e23145.

(23) Yang, Y.; Li, X.; Gu, Y.; Lin, H.; Jie, B.; Zhang, Q.; Zhang, X. Adsorption property of fluoride in water by metal organic framework: Optimization of the process by response surface methodology technique. *Surf. Interfaces* **2022**, *28*, No. 101649.

(24) Guta, M.; Tan, H.; Zhao, Y. Optimization of supercritical CO₂ extraction of incense-enriched oil from *Boswellia papyrifera* resin using response surface methodology. *J. Supercrit. Fluids* **2024**, *205*, No. 106154.

(25) Zhao, L.; Gu, H.; Ye, M.; Wei, M.; Xu, S.; Zuo, X. Optimization of the coupling parameters and mixing uniformity of multiple organic hydraulic mixtures based on the discrete element method and response surface methodology. *Adv. Powder Technol.* **2020**, *31* (10), 4365–4375.

(26) Jedli, H.; Almonnef, M.; Rabhi, R.; Mbarek, M.; Abdessalem, J.; Slimi, K. Activated Carbon as an Adsorbent for CO₂ Capture: Adsorption, Kinetics, and RSM Modeling. *ACS Omega* **2024**, *9* (2), 2080–2087.

(27) Peydayesh, M.; Bagheri, M.; Mohammadi, T.; Bakhtiari, O. Fabrication optimization of polyethersulfone (PES)/polyvinylpyrrolidone (PVP) nanofiltration membranes using Box–Behnken response surface method. *RSC Adv.* **2017**, *7* (40), 24995–25008.

(28) Boondaeng, A.; Vaithanomsat, P.; Apiwatanapiwat, W.; Trakunjae, C.; Janchai, P.; Suriyachai, N.; Kreetachat, T.;

Wongcharee, S.; Imman, S. Biological Conversion of Agricultural Wastes into Indole-3-acetic Acid by *Streptomyces lavenduligriseus* BSS0–1 Using a Response Surface Methodology (RSM). *ACS Omega* **2023**, *8* (43), 40433–40441.

(29) Dhandhi, Y.; Bhardwaj, V.; Naiya, T. K. Application of Novel Biodegradable Demulsifier Synthesized from *Helianthus annuus* in Field Crude Oil Demulsification—Experimental and Modeling Approach through RSM. *Ind. Eng. Chem. Res.* **2023**, *62* (44), 18621–18636.

(30) Luan, W.; Sun, L.; Zeng, Z.; Xue, W. Optimization of a polyvinyl butyral synthesis process based on response surface methodology and artificial neural network. *RSC Adv.* **2023**, *13* (11), 7682–7693.

(31) Watson, M. A.; Tubic, A.; Agbaba, J.; Nikic, J.; Maletic, S.; Molnar Jazic, J.; Dalmacija, B. Response surface methodology investigation into the interactions between arsenic and humic acid in water during the coagulation process. *J. Hazard. Mater.* **2016**, *312*, 150–158.

(32) Zhang, X.; Zhu, X.; Shi, X.; Hou, Y.; Yi, Y. Extraction and Purification of Inulin from Jerusalem Artichoke with Response Surface Method and Ion Exchange Resins. *ACS Omega* **2022**, *7* (14), 12048–12055.

(33) Zhang, T.; Bian, Y.; Wang, L.; Zhao, H.; Wang, G.; Li, C. Continuous Synthesis of Methacrolein over Sulfonic Acid Resin Catalysts: Unraveling the Effect of Acid Strength and Solvent Permittivity. *Ind. Eng. Chem. Res.* **2023**, *62* (33), 12949–12962.

(34) Prabu, G. T. V.; Guruprasad, R.; Sundaramoorthy, C.; Vigneshwaran, N. Process optimization and modelling the BET surface area of electrospun cellulose acetate nanofibres using response surface methodology. *Bull. Mater. Sci.* **2022**, *45* (3), 133.

(35) Fang, Y.; Gu, S.; Liu, S.; Zhang, J.; Ding, Y.; Liu, J. Extraction of oil from high-moisture tuna liver by subcritical dimethyl ether: feasibility and optimization by the response surface method. *RSC Adv.* **2018**, *8* (5), 2723–2732.

(36) Veza, I.; Spraggon, M.; Fattah, I. M. R.; Idris, M. Response surface methodology (RSM) for optimizing engine performance and emissions fueled with biofuel: Review of RSM for sustainability energy transition. *Results Eng.* **2023**, *18*, No. 101213.

(37) Vollmer, N. I.; Driessen, J. L. S. P.; Yamakawa, C. K.; Gernaey, K. V.; Mussatto, S. I.; Sin, G. Model development for the optimization of operational conditions of the pretreatment of wheat straw. *Chem. Eng. J.* **2022**, *430*, No. 133106.

(38) Dipali; Prasad, R.; Sahu, S. K.; Randhawa, N. S. Design and Optimization Study of Metal Recovery from Scrap NdFeB Magnets Using Response Surface Methodology. *Ind. Eng. Chem. Res.* **2023**, *62* (30), 11948–11956.

(39) Guo, Y.; Liu, Z.; Zhang, M.; Tian, X.; Chen, J.; Sun, L. Synthesis and Application of Urea-Formaldehyde for Manufacturing a Controlled-Release Potassium Fertilizer. *Ind. Eng. Chem. Res.* **2018**, *57* (5), 1593–1606.

(40) Li, T. H.; Wang, C. M.; Xie, X. G.; Du, G. B. A computational exploration of the mechanisms for the acid-catalytic urea–formaldehyde reaction: new insight into the old topic. *J. Phys. Org. Chem.* **2012**, *25* (2), 118–125.

(41) Guo, Y.; Shi, Y.; Cui, Q.; Zai, X.; Zhang, S.; Lu, H.; Feng, G. Synthesis of Urea-Formaldehyde Fertilizers and Analysis of Factors Affecting These Processes. *Processes* **2023**, *11* (11), 3251.

(42) Yang, G.; Zhao, H.; Liu, Y.; Li, Z.; Gao, F.; Zhang, Q.; Zou, P.; Liu, Z.; Zhang, M. Slow release fertilizers based on polyphosphate/montmorillonite nanocomposites for improving crop yield. *Arabian J. Chem.* **2023**, *16* (7), No. 104871.

(43) Soleimani, S.; Heydari, A.; Fattahi, M.; Motamedisade, A. Calcium alginate hydrogels reinforced with cellulose nanocrystals for methylene blue adsorption: Synthesis, characterization, and modelling. *Ind. Crops Prod.* **2023**, *192*, No. 115999.

(44) Asfaram, A.; Ghaedi, M.; Agarwal, S.; Tyagi, I.; Kumar Gupta, V. Removal of basic dye Auramine-O by ZnS:Cu nanoparticles loaded on activated carbon: optimization of parameters using response surface methodology with central composite design. *RSC Adv.* **2015**, *5* (24), 18438–18450.

(45) Djimtoingar, S. S.; Derkyi, N. S. A.; Kuranchie, F. A.; Yankyera, J. K. A review of response surface methodology for biogas process optimization. *Cogent Eng.* **2022**, *9* (1), No. 2115283.

(46) Mansour, R.; Ezzili, B.; Farouk, M. The use of response surface method to optimize the extraction of natural dye from winery waste in textile dyeing. *J. Text. Inst.* **2017**, *108* (4), 528–537.